

RSC Advances



This is an *Accepted Manuscript*, which has been through the Royal Society of Chemistry peer review process and has been accepted for publication.

Accepted Manuscripts are published online shortly after acceptance, before technical editing, formatting and proof reading. Using this free service, authors can make their results available to the community, in citable form, before we publish the edited article. This *Accepted Manuscript* will be replaced by the edited, formatted and paginated article as soon as this is available.

You can find more information about *Accepted Manuscripts* in the [Information for Authors](#).

Please note that technical editing may introduce minor changes to the text and/or graphics, which may alter content. The journal's standard [Terms & Conditions](#) and the [Ethical guidelines](#) still apply. In no event shall the Royal Society of Chemistry be held responsible for any errors or omissions in this *Accepted Manuscript* or any consequences arising from the use of any information it contains.

Realization of a fast-response flexible ultraviolet photodetector employing metal-semiconductor-metal structure InGaZnO photodiode

H. T. Zhou^a, L. Li^{a,*}, H. Y. Chen^b, Z. Guo^c, S. J. Jiao^d, W. J. Sun^a

^aKey Laboratory for Photonic and Electronic Bandgap Materials, Ministry of Education, School of Physics and Electronic Engineering, Harbin Normal University, Harbin 150025, PR China

^bDepartment of Materials Science, Fudan University, Shanghai 200433, People's Republic of China

^cCAS Key Lab of Bio-Medical Diagnostics, Suzhou Institute of Biomedical Engineering and Technology, Chinese Academy of Sciences, No. 88, Keling Road, Suzhou New District 215163, People's Republic of China

^dSchool of Materials Science and Engineering, Harbin Institute of Technology, Harbin 150001, PR China

Amorphous InGaZnO (a-IGZO) thin films have been grown on polyethylene terephthalate (PET) substrates using plasma-assisted pulsed laser deposition (PLD) technique, and a flexible ultraviolet (UV) photodetector (PD) with a simple metal-semiconductor-metal (MSM) structure was prepared on the a-IGZO films. The flexible PD shows relatively good photoresponse characteristics before and after bending, and keeps good folding reproducibility after repeated bending up to 500 cycles. More importantly, it shows fast speed with response and recovery time of 0.8 ms and 2.0 ms, 33.8 ms, which is much faster than that of the reported flexible ultraviolet detectors. The devices reported in this paper provide an optimal way to realize flexible ultraviolet detector with fast speed.

Introduction

UV PDs have a wide range of potential applications in missile plume detection, secure communication, flame alarm, and environmental pollution monitoring.¹⁻⁴ Recently, great interests have been focused on flexible PDs due to the foldable, wearable, lightweight and portable characteristics as compared to conventional rigid PDs. Until now, the reports on flexible ultraviolet detectors often employ 1D inorganic nanostructure, but their preparation process are complex, which includes

* Corresponding author.
E-mail addresses: physics_lin@hotmail.com;

high temperature synthesis ($>800\text{ }^{\circ}\text{C}$) for guarantee of high crystalline and high field assisted assembly process and so on.⁵⁻¹⁰ In general, the large surface-to-volume ratio of 1D nanostructure can significantly increase the number of surface trap states and prolong the photo carriers' lifetime, then the UV PDs based on 1D nanostructure generally show big photoconductive gain.¹¹ Unfortunately, they sacrifice response speed of PDs, the typical range of the response time is from several seconds to several hours.⁵⁻¹⁰ As one of the key factors for detection performance, response speed determines the capability of the device to follow optical signals that can be utilized in optical switch and light wave communication fields. So, realizing a flexible UV PDs that have a fast response speed will naturally broaden the scope of the device application.

The a-InGaZnO film has been widely pursued for decades due to the wide applications in transparent thin film transistors (especially on flexible substrates), photodetectors, and so on.^{12,13} Benefiting from its superior features over other semiconductors including room temperature (RT) process availability, good-uniformity for large area, wide band gap ($> 3.0\text{ eV}$) and high electron mobility ($1\sim 30\text{ cm}^2/\text{Vs}$ at RT), it has also been used to fabricate UV detectors.¹²⁻¹⁹ However, the device structure is mainly focused on the complicated transistor structure. In particular, MSM photodiodes are a family of fast, high-sensitivity detectors. Their simple planar structures enable easy fabrication in a process compatible with planar circuit technology. Thus, these devices are attractive candidates for using in integrated optoelectronic-electronic systems. If a flexible a-IGZO UV detector with high response speed based on simple MSM structure was realized, it will have extensive commercial applications. Till now, a flexible a-IGZO UV detector based on simple MSM structure has not been reported yet.

In this paper, a flexible a-IGZO UV PD has been fabricated based on simple MSM structure at RT. The UV PD shows relatively good photoresponse characteristics under bend condition, and keeps good folding reproducibility after repeated bending up to 500 cycles. Most importantly, the flexible UV PD shows a fast response speed, the rise time and decay time are 0.8 ms and 2.0 ms, 33.8 ms, respectively, which are

quite outstanding values in light of previously flexible detectors. Our experiments provide an optimal way to obtain high speed flexible UV PD.

Experimental details

The a-IGZO films were grown on PET substrates and *c*-plane sapphire substrates by PLD technique, respectively. The substrates were sequentially cleaned with acetone, ethanol and deionized water in an ultrasonic bath for 15min, respectively. After being cleaned, the substrates were blown dry using high purity nitrogen gas (purity > 99.99%). Before the deposition, the growth chamber was pumped to a vacuum degree below 6.0×10^{-5} Pa with a turbo molecular pump. Then, the high purity oxygen gas (99.99%) was introduced into the chamber. The oxygen flow was fixed at 20 sccm, and a Nd: YAG (Quantel Brilliant B) pulsed laser ($t_s = 5$ ns, $\lambda = 355$ nm, laser energy = 170 mJ/pulse, repetition rate = 10 Hz) was employed to ablate an IGZO target (In: Ga: Zn = 1:1:1, purity > 99.99%) in an oxygen partial pressure of 2.0 Pa during the growth process. The a-IGZO films were deposited at RT for 2 hours. The morphology of the sample was characterized using a Hitachi SU70 scanning electron microscope (SEM). The crystalline property of the film was analyzed by X-ray diffractometer (XRD). The optical absorption spectrum was recorded using ultraviolet-visible spectrophotometer.

Gold film (60 nm thick) was deposited by the vacuum thermal evaporation technique. 12 pairs of interdigital electrodes with 5 μm width, 10 μm gap, and 500 μm length, were configured onto the a-IGZO layer through the photolithography and wet etching process. The current-voltage (*I-V*) characteristic of the PD was measured using the Agilent B1500A semiconductor device analyzer. The photoresponse characteristic (Zolix DR800-CUST) of the PD was measured at RT. The temporal response of the device was measured using a pulsed Nd:YAG laser (355 nm, 10 ns) as the excitation source.

Results and discussion

Fig. 1 shows the XRD pattern of the IGZO film grown on *c*-sapphire at the same

growth process with the film grown on the PET substrates. Besides the diffraction from the sapphire substrate, there is no other obvious diffraction peak of crystalline phase in the pattern, indicating the IGZO film is amorphous phase. The typical cross-sectional SEM image of the a-IGZO films is shown in the inset of Fig. 1a. It can be seen that the thickness is about 172 nm. Fig. 1b shows the absorption spectrum of the a-IGZO thin film, which exhibits a strong UV absorption. The relationship between the Tauc plot of $(\alpha h\nu)^{1/2}$ and the photon energy $h\nu$ (α absorption coefficient) in the a-IGZO film is shown in its inset image. The optical bandgap of the a-IGZO film can be derived to be around 3.18 eV by extrapolating the linear portion of the plot to the photon energy axis. Fig. 2a shows the photoresponse characteristic of the PD under illumination condition at zero bias. It can be obvious seen that the responsivity of the PD is about 0.1 mA/W, and the peak response wavelength is located at 350 nm. The zero-bias photoresponse characteristic of the MSM structure IGZO has been found in our previous report,¹³ which is attributed to an asymmetric Schottky barriers formed at the two sides of the Au/a-IGZO interdigital electrodes where the carrier-trapping process occurred in metal electrode (Au)/semiconductor (a-IGZO) interface. As shown in Fig. 2b, the I - V characteristics of the flexible UV PD under 310 nm light illumination with a power density of 0.76 mW/cm² and a dark condition were shown in Fig. 2b. It can be clearly seen that the photocurrent (red) is 10²~10³ times larger than the dark current (black) under the bias. Meanwhile, a clear Schottky behavior can be observed in the I - V curve (black) under dark condition, which comes from the Au/a-IGZO interfaces, in order to understand the formation of the Schottky behavior, and the scheme of the band alignment between them can be found in Fig. 2c. Furthermore, an obvious asymmetric shape in the plus and minus voltage can be seen in the I - V curve under dark condition, which also indicate that the asymmetric Schottky barriers were formed at the two sides of the Au/a-IGZO interdigital electrodes in our flexible UV PD, the formation mechanism of the asymmetric Schottky barriers can be found in our previous reports.¹³

The photo sensitivity linearity (typically quoted in dB) LDR is one of the important figure-of-merits for a photodetector and can be given by the following

equation^{24,25}

$$\text{LDR} = 20\log(I_{ph}^*/I_d) \quad (1)$$

Where I_{ph}^* is the photocurrent, measured at light intensity of mW/cm^2 , I_d is the dark current. As shown in Fig. 2b, the LDR value increases to the highest value of 70.17 dB at 2 V, and then decreases as the voltage increasing.

To demonstrate the photoresponse characteristics of our flexible UV PD, a series of biases have been applied onto the flexible UV PD, and the photoresponse spectra under different biases have been recorded, as shown in Fig. 2d. It can be clearly seen that the device shows a good photosensitivity for ultraviolet light. The responsivity of the PD is 0.77 A/W at 14 V bias, and the ultraviolet/visible rejection ratio ($R_{330\text{ nm}}/R_{450\text{ nm}}$) of more than two orders of magnitude was obtained in our flexible PD. The inset of Fig. 2d shows the responsivity of the flexible UV PD as a function of bias voltage. A nonlinear relationship of responsivity is observed from 0 V (0.1 mA/W) to 14 V (770 mA/W), which indicates that no carrier mobility saturation or sweep-out effect occurs up to 14 V bias in our flexible device.²⁰ The detectivity (D^*) is one of the key figure-of-merits for a photodetector, which usually describes the smallest detectable signal.^{24,25} The detectivity of a photodetector can be determined by $D^* = R_\lambda/(2eJ_d)^{1/2}$, where R_λ is the responsivity of the photodetector, e is the elemental charge, and J_d is the dark current density.^{24,25} It is a parameter that can comprehensively evaluate the responsivity and dark current. As shown in Fig. 2b and Fig. 2d, the responsivity of the 0.45 A/W and the dark current of 2.62×10^{-8} A at 10 V bias indicate the detectivity get the maximum value with $2.08 \times 10^{13} \text{ cm}\cdot\text{Hz}^{1/2}/\text{W}$ (Jones).

Next, in order to check the practical application of the flexible UV PD, bending effects on the photoresponse characteristics were examined. Fig. 3a shows the photoresponse characteristics of the flexible UV PD at 2 V bias under various bending angles. To clearly demonstrate the influence of bending angles on responsivity of the flexible UV PD, the dependence of the responsivity at different bending angles was shown in the inset of Fig. 3a. It can be seen that the responsivity of the PD gradually decreased with the bending angles increasing, and the responsivity decreased to 50%

when the bending angle is up to 50° , the obvious decay of responsivity under bending condition could be attributed to the reason that free electrons were trapped by the bending-strain-induced defects.⁹ The folding endurance is also a key parameter for the application of the flexible devices. The photoresponse characteristics of the flexible UV PD with respect to repeated mechanical bending are further recorded in Fig. 3b. The photoresponse characteristic almost remains unchanged after repeated bending up to 500 cycles (Bending of the device from 0° to 50° followed by releasing of it back to 0° was considered as one cycle), which indicate that our flexible UV PD has good folding reproducibility.

As well known, the response speed is a predominant parameter in practical applications to evaluate the performance of detector under a quickly varying optical signal. To test the response speed of our a-IGZO UV PDs, the response rise time and the decay time of the flexible UV PD were measured in air. Fig. 4a shows the pulse response data of the devices. The response time of the PDs is about 0.8 ms which is estimated as the 10–90% rise time, and the decay edge can be well fitted to a second-order exponential decay function, with two time constants of 2.0 ms and 33.8 ms, as shown in Fig. 4b. Compared to other flexible devices, our photodetector has fast response performance. For example, a flexible hybrid photodetector (PPani/TiO₂) possesses the rise time of 22.87 ms and the decay time of 34.23 ms.²¹ The photocurrent rise and decay time of In₂Ge₂O₇ nanowire mats based flexible device are about 15000 ms and 1000 ms,⁶ respectively. As one of the key factors for detection performance, the relatively faster response time can naturally broaden the scope of the device application. In our case, fast response could be due to high electron mobility in the a-IGZO film, and an asymmetric Schottky barrier formed at the two sides of the Au/a-IGZO interdigital electrodes and so on. Compared with the flexible UV PD based on 1D nanostructure, rapid recovery rate in our PD is mainly due to the relative low surface trap states, which traps little photo-generated holes.¹¹ In order to clearly observe the comparison of typical photodetecting performance of our flexible UV PDs and some reported UV PDs. Table 1 summarizes progress in these figure-of-merits of some flexible UV PDs and traditional UV PDs. Compare with the

UV PDs, our flexible UV PD has good photodetecting performance, more important, our device has fast response speed.

Conclusion

The flexible UV PD based on simple MSM structure has been fabricated based on a-IGZO film. The PD shows relatively good photoresponse before and after bending, excellent folding endurance. Importantly, the flexible UV PD shows fast response characteristics with response rise time of 0.8 ms and response decay time of 2.0 ms and 33.8 ms, which is much faster than that of the reported flexible UV PDs. The fast response characteristic should be attributed to the synergistic effect of multiple factors, such as the high electron mobility in a-IGZO film, an asymmetric Schottky barrier formed at the two sides of the Au/a-IGZO interdigital electrodes, and low surface trap states of a-IGZO film compared with 1D nanostructures and so on. Our results demonstrate that the flexible a-IGZO UV PD can be applied in flexible optoelectronics, especially in the flexible device field needing fast response speed.

Acknowledgements

This work was supported by the Natural Science Foundation of China (Grant No. 61404039 and 51202154), Heilongjiang Province Foundation for Returned Chinese Scholars (Grant No. LC201401), Educational Commission of Heilongjiang Province of China (Grant No. 12531Z006), the Natural Science Foundation of Jiangsu Province under Grant Nos. BK20131169, and the Graduate Student's Scientific Research Innovation Project of Harbin Normal University (HSDSSCX2015-01).

References

- 1 D. B. Li, X. J. Sun, H. Song, Z. M. Li, H. Jiang, Y. R. Chen, G. Q. Miao and B. Shen, *Appl. Phys. Lett.*, 2011, **99**, 261102.
- 2 H. Zhu, C. X. Shan, L. K. Wang, J. Zheng, J. Y. Zhang, B. Yao and D. Z. Shen, *J. Phys. Chem. C*, 2010, **114**, 7169–7172.
- 3 Y. Z. Jin, J. P. Wang, B. Q. Sun, J. C. Blakesley and N. C. Greenham, *Nano Lett.*, 2008, **8**, 1649-1653.

- 4 J. S. Liu, C. X. Shan, B. H. Li, Z. Z. Zhang, C. L. Yang, D. Z. Shen and X. W. Fan, *Appl. Phys. Lett.*, 2010, **97**, 251102.
- 5 J. M. Wu, Y. R. Chena and Y. H. Linb, *Nanoscale*, 2011, **3**, 1053–1058.
- 6 Z. Liu, H. T. Huang, B. Liang, X. F. Wang, Z. R. Wang, D. Chen and G. Z. Shen, *Opt. Express*, 2012, **20**, 2982-2991.
- 7 S. Bai, W. W. Wu, Y. Qin, N. Y. Cui, D. J. Bayerl and X. D. Wang, *Adv. Funct. Mater.*, 2011, **21**, 4464–4469.
- 8 B. A. Manekkathodi, M.-Y. Lu, C. W. Wang and L.-J. Chen, *Adv. Mater.*, 2010, **22**, 4059–4063.
- 9 K. W. Liu, M. Sakurai, M. Aono and D. Z. Shen, *Adv. Funct. Mater.*, 2015, **10** 1002.
- 10 W. Tian, C. Zhang, T. Y. Zhai, S. L. Li, X. Wang, J. W. Liu, X. Jie, D. Q. Liu, M. Y. Liao, Y. Koide, D. Golberg and Y. Bando, *Adv. Mater.*, 2014, **26**, 3088–3093.
- 11 X. F. Wang, Y. Zhang, X. M. Chen, M. He, C. Liu, Y. A. Yin, X. S. Zou and S. T. Li, *Nanoscale*, 2014, **6**, 12009–12017.
- 12 K. C. Ok, S. H. K. Park, C. S. Hwang, H. Kim, H. S. Shin, J. Bae and J. S. Park, *Appl. Phys. Lett.*, 2014, **104**, 063508.
- 13 D. L. Jiang, L. Li, H. Y. Chen, H. Gao, Q. Qiao, Z. K. Xu and S. J. Jiao, *Appl. Phys. Lett.*, 2015, **106**, 171103.
- 14 H. H. Hsieh, T. Kamiya, K. Nomura, H. Hosono and C. C. Wu, *Appl. Phys. Lett.*, 2008, **92**, 133503.
- 15 A. Takagi, K. Nomura, H. Ohta, H. Yanagi, T. Kamiya, M. Hirano and H. Hosono, *Thin Solid Films*, 2005, **486**, 38–41.
- 16 H. W. Zan, W. T. Chen, H. W. Hsueh, S. C. Kao, M. C. Ku, C. C. Tsai and H. F. Meng, *Appl. Phys. Lett.*, 2010, **97**, 203506.
- 17 T. H. Chang, C. J. Chiu, S. J. Chang, T. Y. Tsai, T. H. Yang, Z. D. Huang and W. Y. Weng, *Appl. Phys. Lett.*, 2013, **102**, 221104.
- 18 T. H. Chang, C. J. Chiu, W. Y. Weng, S. J. Chang, T. Y. Tsai and Z. D. *Appl. Phys. Lett.*, 2012, **101**, 261112.
- 19 C. J. Wu, X. F. Li, J. G. Lu, Z. Z. Ye, J. Zhang, T. T. Zhou, R. J. Sun, L. X. Chen,

- B. Lu and X. H. Pan, *Appl. Phys. Lett.*, 2013, **103**, 082109.
- 20 W. Yang, R. D. Vispute, S. Choopun, R. P. Sharma and T. Venkatesana, *Appl. Phys. Lett.*, 2011, **78**, 2787.
- 21 A. A. Hussain, A. R. Pal and D. S. Patil, *Appl. Phys. Lett.*, 2014, **104**, 193301.
- 22 A. M. Selman and Z. Hassan, *Sensors and Actuators A*, 2015, **221**, 15–21.
- 23 W. Dai, X. H. Pan, S. S. Chen, C. Chen, W. Chen, H. H. Zhang and Z. Z. Ye, *RSC Adv.*, 2015, **5**, 6311.
- 24 B. Zhao, F. Wang, H. Y. Chen, Y. P. Wang, M. M. Jiang, X. S. Fang and D. X. Zhao, *Nano Lett.*, 2015, **15**, 3988–3993.
- 25 X. Liu, L. I. Gu, Q. P. Zhang, J. Y. Wu, Y. Z. Long, and Z. Y. Fan, *Nat. Commun.*, 2014, **5**, 4007.

Figures caption:

Fig. 1 (a) XRD pattern of IGZO film deposited on sapphire substrate by PLD, the typical cross-sectional (inset) SEM image of the film. (b) The absorption spectrum of the a-IGZO film grown on sapphire substrate, the inset shows the band gap of the a-IGZO film.

Fig. 2 (a) The photoresponse characteristic of the flexible UV PD at 0 V bias, and the inset shows a schematic illustration of the MSM structure. (b) The I - V characteristic of the flexible a-IGZO photodetector under dark and illumination with 310 nm light of 0.76 mW/cm^2 . Inset: the I - V curve under dark conduction in first quadrant. (c) The scheme of the band alignment between a-IGZO film and Au electrodes. (d) The photoresponse spectra of the flexible UV PD as a function of the incident light wavelength under different bias, and the inset shows the responsivity as a function of bias voltage.

Fig. 3 (a) The photoresponse spectra of the flexible UV PD as function of incident light with different bending angles under 2 V bias. The inset shows decay tendency of

the responsivity of the flexible UV PD under different bending angles. (b) Typical photoresponse spectra of the device after different folding cycles under 2 V bias

Fig. 4 (a) The temporal response of the flexible UV PD at 5V bias excited by 355 nm Nd:YAG laser pulses in air. (b) The temporal response spectrum of the PD in a single on/off cycle.

Table I Comparison of typical photodetecting performance of some flexible UV PDs and traditional UV PDs.

Fig. 1.

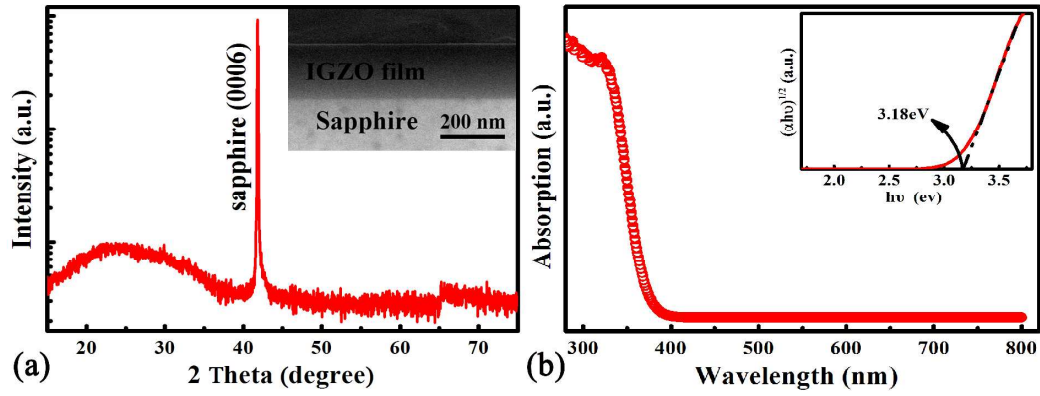


Fig. 2.

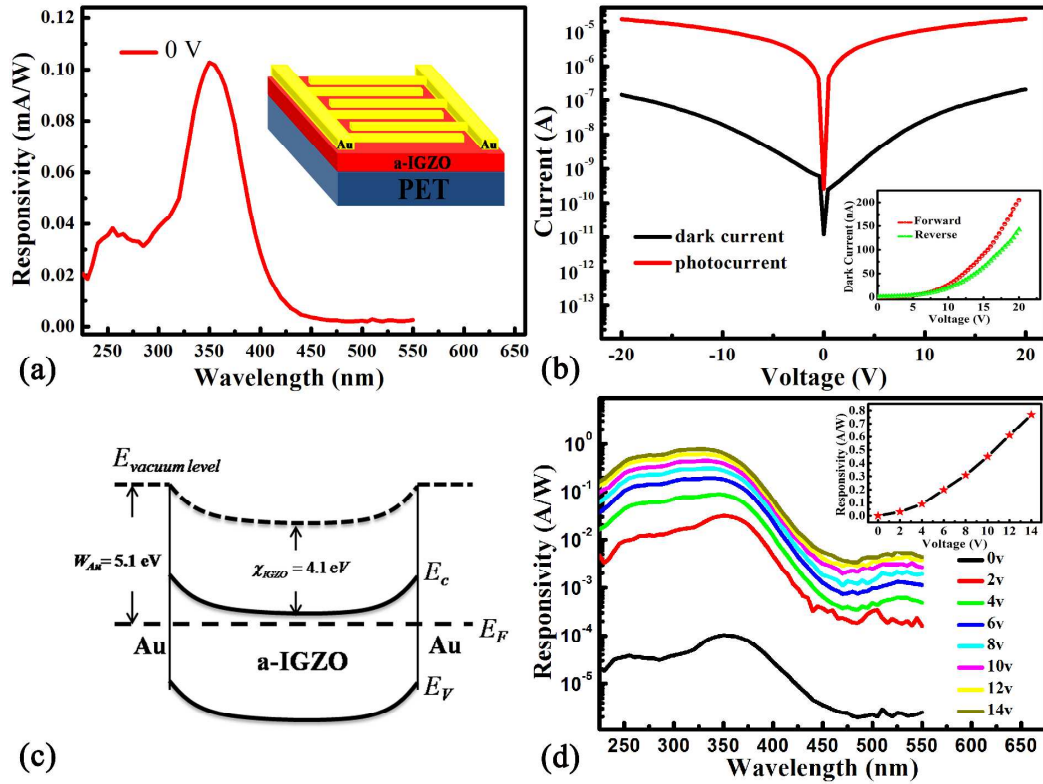


Fig. 3.

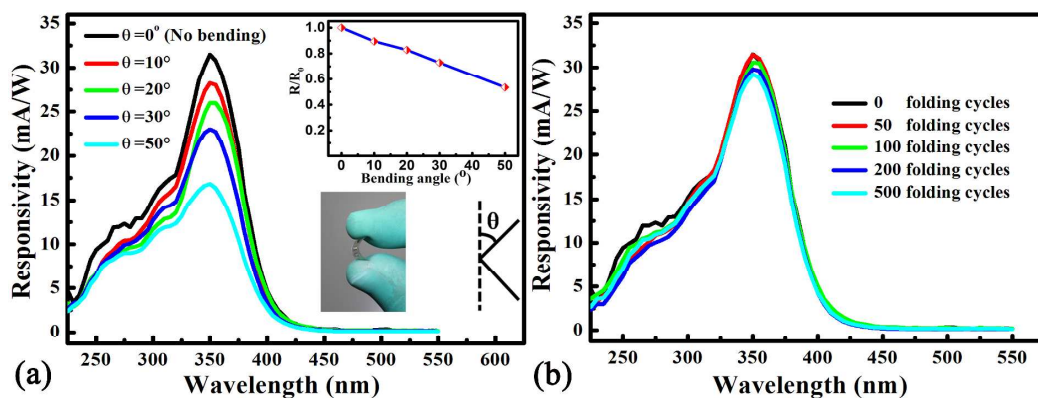


Fig. 4.

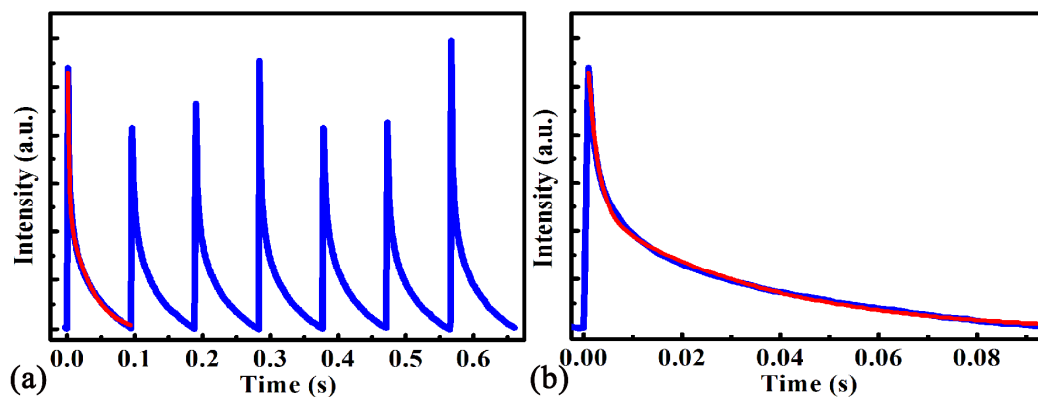


Table I

	PD (ref.)	Bias(V)/Wavelength(nm)/Intensity(mW/cm ²)	I _{photo} (A)	I _{dark} (A)	LDR (dB)	D* (Jones)	RT (s)	DT (s)
Flexible	Zn ₂ GeO ₄ nanowire ⁶	15/254/0.85	0.87×10^{-9}	0.29×10^{-11}	-	-	~2.5 s	<1 s
	SnO ₂ microrod ⁹	2/260/0.5 $\times 10^{-4}$	4.40×10^{-5}	2.60×10^{-5}	-	-	-	<1 s
	ZnS/ZnO Heterostructure ¹⁰	10/320/0.2	3.29×10^{-11}	5.30×10^{-12}	-	-	0.77 s	0.73 s
	PPani-TiO ₂ film ²¹	5/254/0.06	1.01×10^{-4}	0.11×10^{-6}	-	-	2.287×10^{-2}	3.423×10^{-2}
	InGaZnO MSM structure (This work)	2/310/0.76	1.78×10^{-6}	5.69×10^{-10}	70.17	2.08×10^{13}	8×10^{-4}	2.0×10^{-3}, 3.38×10^{-2}
Traditional	TiO ₂ nanorod array ²²	5/325/1.6	6.09×10^{-4}	1.27×10^{-4}	-	-	5.08×10^{-2}	5.78×10^{-2}
	ZnO Homojunction ²³	-3/365/-	-	2.83×10^{-5}	-	-	15.2 s	7.3 s, 20.3 s
	ZnO/Ga ₂ O ₃ Microwire ²⁴	-6/254/1.67	-	5.35×10^{-10}	119.3	9.91×10^{14}	2.0×10^{-5}	0.32 s
	ZnO nanowire ²⁵	1v/365/0.5 $\times 10^{-6}$	4.8×10^{-11}	2.7×10^{-11}	114	3.3×10^{17}	-	-